

Crack front propagation by kink formation

Frohmut Rösch and Hans-Rainer Trebin

Institut für Theoretische und Angewandte Physik, Universität Stuttgart, Pfaffenwaldring 57, 70550 Stuttgart, Germany

Fracture of a three-dimensional brittle solid generates two-dimensional surfaces, which are formed behind a one-dimensional crack front. For *quasi-static* cracks on a (111) cleavage plane in silicon front propagation by kink-pair formation was proposed and proven by a reaction-pathway analysis with Stillinger-Weber potentials. Here, we demonstrate that the kink-pair mechanism is much more general: We also observe it in molecular *dynamics* simulations of a complex metallic alloy, the C15 NbCr₂ Friauf-Laves phase, where we applied carefully selected embedded-atom-method potentials. The numerical experiments highlight that kink formation is essential for crack propagation in any brittle material.

Introduction

In a brittle material a travelling crack generates an upper and a lower fracture surface, which meet at a one-dimensional crack front. From a macroscopic point of view there is no reason why this curve should deviate from a straight line, contrary to the atomistic point of view, where a crack propagates by successive rupture of cohesive bonds. Here we demonstrate that breakage of these bonds leads to kinks in the front, similar to solitons in dislocations [1, 2].

The atomistic origin of fracture also leads to the lattice trapping effect [3], which shows up in deviations from the Griffith criterion [4]. This criterion is based on an energy balance. The elastic energy stored in the system has to be sufficient for the creation of the fracture surfaces. However, due to the discreteness of the lattice, a crack is stable in an entire interval around the Griffith load. Thus, cracks in general start to propagate only at loads above the predictions of the Griffith criterion.

A further consequence of the discrete nature of matter is a strong directional dependence of crack velocity and roughness of the cleavage plane [5–7].

Many previous atomistic simulations either were performed in two-dimensional systems or in three-dimensional samples under plane-strain conditions, where periodic boundary conditions apply along the crack front. Typically, only one atomic spacing or one unit cell is used in this direction for repetition representing a quasi-two-dimensional situation, which impedes an unrestricted movement of the crack front. In silicon, however, a minimum energy path in *three* dimensions for a series of bond ruptures was determined [8, 9]. A reaction pathway analysis with Stillinger-Weber potentials was performed between an initial and a final state, which represented perfectly straight crack lines in local equilibrium. It was found that the crack front extension occurs through a kink mech-

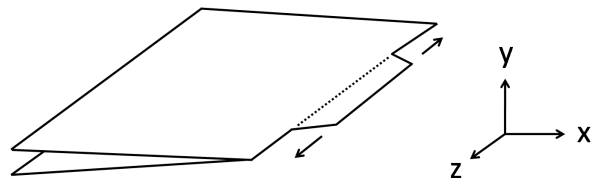


Fig. 1: Schematic drawing of a crack, which advances by a kink-pair mechanism.

anism. In this quasi-static approach, the crack cannot deviate from its cleavage plane. Dynamic aspects and effects of the overload due to the lattice trapping are not taken into account.

They can be taken into regard by molecular *dynamics* simulations. In silicon these suffer from the fact that simple interatomic interactions lead to questionable results [10–13]. The kink-pair mechanism¹, however, resulting from the quasi-static simulations (see Fig. 1), could be relevant and observable for any ordered brittle system [14, 15]. We have checked it for a system where very reliable interaction potentials are available.

Method

Molecular dynamics simulations were performed on a brittle intermetallic compound to investigate dynamic crack propagation at low temperature in detail. The chosen complex metallic alloy NbCr₂ forms one of the Friauf-Laves phases, which represent the largest subset of topologically close-packed intermetallic compounds [16]. The choice of a metallic system avoids problems with the interactions. The potentials for the Friauf-Laves phase were de-

¹The authors of Ref. [8] called the effect “double-kink mechanism”, but the notion “kink-pair mechanism” is more appropriate (compare e.g. Fig. 1 of [1]).

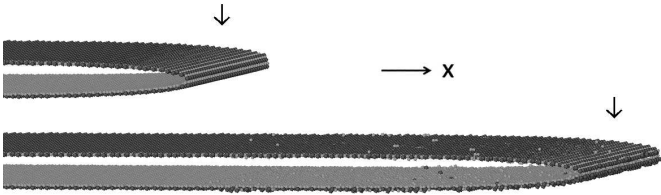


Fig. 2: Atoms forming the fracture surfaces ($k = 1.15$). Top: $t = 0$, bottom: $t = 102$ ps. Dark (bright) spheres indicate Nb (Cr) atoms.

rived from ab-initio calculations and were carefully tested and validated [6, 17] for the purpose of fracture simulations. As the Nb atoms form a diamond lattice which is filled by a tetrahedral network of Cr atoms, there is also a loose relationship to the structure of silicon. With 24 atoms in the cubic unit cell, C15 NbCr₂ is structurally already quite complex. The simulation cells contain about 5 million atoms with dimensions of approximately $l \times \frac{l}{3} \times \frac{l}{6}$, where $l \approx 0.1 \mu\text{m}$ is the length in crack propagation direction (x -axis). Larger scale (≈ 20 nm) periodic boundary conditions apply along the crack front (z -direction). Details of the simulation technique for a mode I crack already were published and can be found elsewhere [5, 6, 18, 19].

Results and discussion

A crack orientation of lowest Griffith load is chosen, where the resulting fracture surfaces are expected to show minute roughening [6, 7]. A crack is driven in the $[2\bar{1}1]$ direction on a (111) plane. The position of the initial seed crack differs from previously published data [7], which concentrated on more macroscopic effects such as crack speed and surface roughness. The fracture surface is visualised by plotting only atoms with reduced coordination, as shown in Fig. 2. The seed crack (top) is displayed together with a snapshot after 102 ps (bottom) for $k = 1.15^2$. Nearly perfect brittle cleavage is observed. The surplus of energy due to $k > 1$ results in some imperfections. Thus, the lattice trapping can lead to non-equilibrium fracture surfaces. Hence, in general, fracture surfaces are *not* explicitly those of lowest energy or lowest roughness. Furthermore, due to the dynamic process, the crack tip heats up and acoustic waves are emitted from the crack line as atomic bonds break [5, 20, 21].

Atoms forming the fracture surfaces are projected onto the x - z -plane (following the arrows in Fig. 2). The crack front is obtained by scanning this data with a sphere of radius 0.5 nm. Corresponding configurations are shown in Fig. 3 for $k = 1.1$ for a selected time-sequence. The pictures are snapshots from a movie (available online). The steady-state motion of the propagating crack ($v_I = 0.11$

²The external load of a system is contained in the stress intensity factor K . The reduced stress intensity factor k is defined as K in units of the Griffith value K_{Griffith} : $k = K/K_{\text{Griffith}}$.

km/s) has been subtracted to fix the view on the crack front (see arrows in Fig. 2). The main characteristic of the advancing front is the lateral movement of two kinks [indicated by arrows in Fig. 3 a)-e)], which annihilate when they meet [f)].

The crack front extension d in x -direction is given by the difference of the maximal and minimal x value of the line: $d = x_{\text{max}} - x_{\text{min}}$. As long as kinks move by sidewise motion to advance the crack a certain distance in x -direction, d remains constant. For a straight line d vanishes. As the crack line is generated by scanning atoms with a sphere, however, d always will take values above a small but finite threshold. The selection of atoms according to their coordination number within a certain shell also will make single atoms emerge or vanish along the crack front [see e.g. Fig. 3 d), $z \approx 7$ nm and $z \approx 14.5$ nm]. Both aspects influence d , which is plotted in Fig. 4 against time (solid line: $k = 1.1$). The configurations b)-e) shown in Fig. 3 have $d_{\text{max}} \approx 0.6$ nm. For $t = 13.6$ ps, d drops to a value d_{min} below 0.2 nm. This sequence of nearly constant maximal values d_{max} with certain drops to small values d_{min} is the signature of kink motions as described above. It is repeating as can be seen from Fig. 4. The non-periodic fashion of repetition shows that additional effects play a role. Indeed, after about 25 ps the crack is arrested and does no longer propagate for $k = 1.1$ (see online movie). Crack propagation also resulted in out-of-plane movement, effectively roughening the fracture surface. The energy stored in the system then does no longer suffice to create these rough surfaces in steady state motion. The crack front is stuck and straightens ($d \approx d_{\text{min}}$) due to the applied load (see Fig. 4).

The main difference to a quasi-static motion is the dissipation of energy close to the crack front. Local heating, acoustic emissions and the creation of rough surfaces influence crack propagation. From atomistic simulations it is known that cracks propagate only above a minimal non-zero value of the steady state crack velocity. This is interpreted as the consequence of rapidly snapping bonds [22]. When cracks propagate too slow, too much energy is dispersed from the crack front by phonons before the crack arrives at the next bond. Thus, at a critical velocity, no further bonds will break, and at low loads, any disturbance from the steady state propagation may effectively influence and even stop an advancing crack front.

How do the kinks evolve? Along the crack front of an atomically sharp seed crack no bond differs significantly from the others at low temperature and low load. Kinetic and potential energy of the atoms are almost evenly distributed and not sufficient to initiate rupture. Only above a certain threshold the bonds break more or less simultaneously³ and the crack starts to propagate. Thus, for short times t , d lies well below d_{max} . The bond strengths and the properties of the atoms close to the crack front change after crack motion due to local heating, acoustic

³within the time-resolution chosen by observation

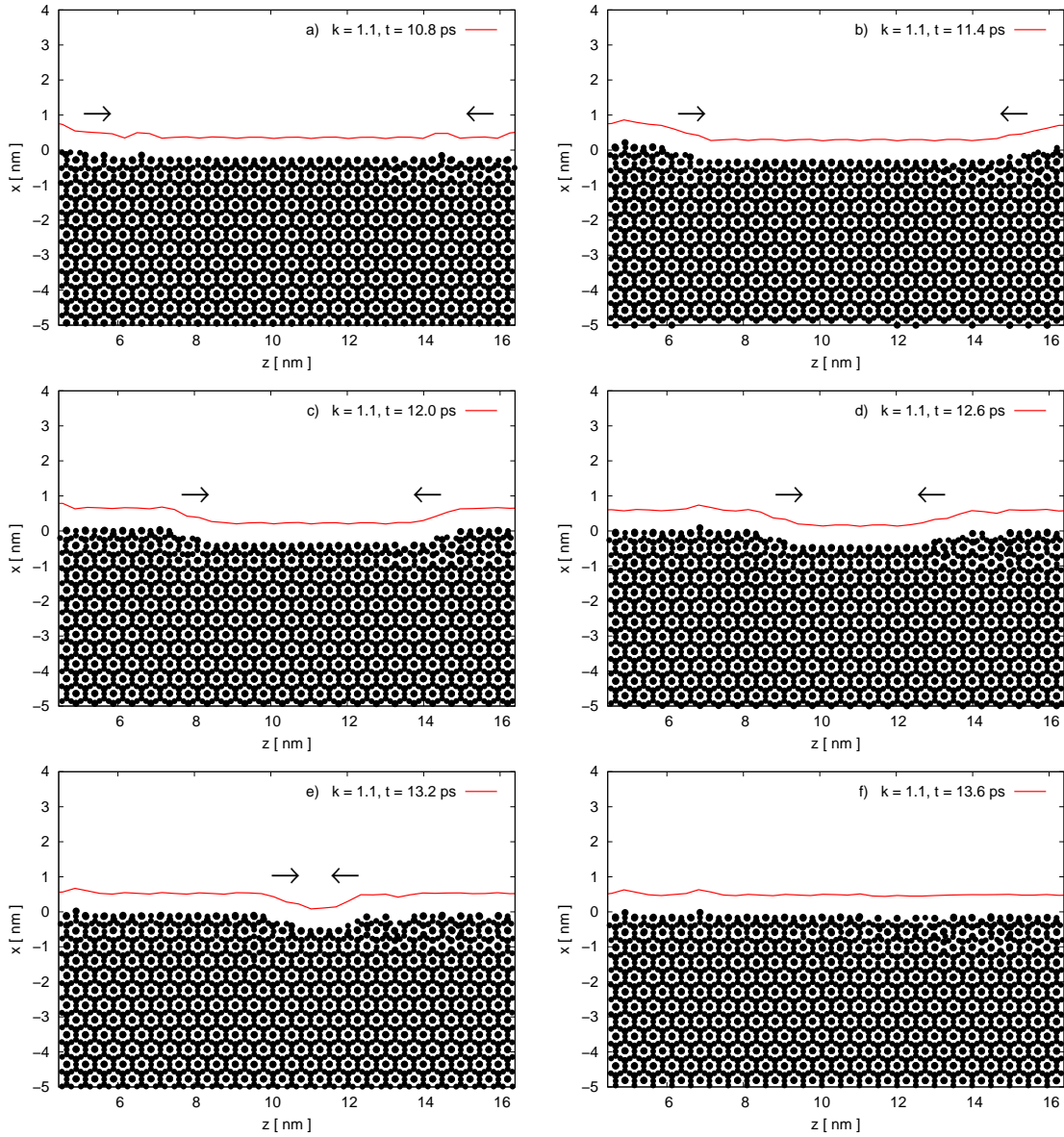


Fig. 3: Crack advancing by a kink-pair mechanism ($k = 1.1$, $t = 10.8$ ps ... 13.6 ps).

emissions and roughening. The weakest bonds will break first and will decimate the neighbouring linkings. These will rupture subsequently. Thus, the crack front propagates by sequentially breaking bonds in a sidewise motion, which is equivalent to the kink-pair mechanism shown in Fig. 1. As dynamic fracture is a non-equilibrium process, details deviate from this simple picture. However, at least for $k = 1.1$, the significance of the kink mechanism for dynamic fracture is evident.

What happens at higher loads? The crack front extension d is plotted for $k = 1.3$ in Fig. 4 (dashed line). Compared to the values for $k = 1.1$, $d > d_{\max}$ is observable. Furthermore, there is more scatter in the data, which also looks less regular. For $t = 46.4$ ps a projection of the crack as in Fig. 3 is displayed in Fig. 5 with $d \approx 2d_{\max}$. More

than a single kink-pair mechanism is occurring. Furthermore, the fracture surfaces are rougher, which is obvious from the faults in Fig. 5 in contrast to Figs. 3. Thus, both the in-plane and the out-of-plane roughness increase. Although kinks can be seen in the crack front, the behaviour is more complicated than for the lower load. The crack now propagates at a significantly higher velocity $v_{II} = 1.04$ km/s. For this motion another online movie is available. As is evident from Figs. 5 and 4 also for higher loads the crack front in general deviates from a straight line. The increased roughness can be seen as an analog of the macroscopic mirror-mist-hackle regions on an atomic scale. Energy is dissipated by heating the sample, by emission of radiation and by increasing the roughness of the fracture surfaces and thus the surface energy. It was observed that

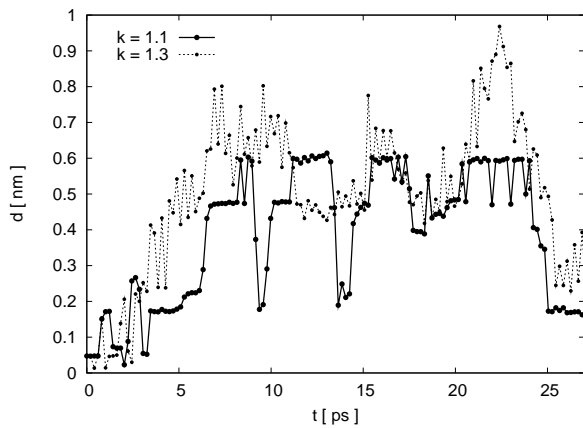


Fig. 4: Crack front extension.

cracks tend to create upper and lower fracture surfaces of similar energy when roughening occurs [7,23]. Bending of the crack front is not restricted to the atomic level. In more complex systems like quasicrystals, containing clusters [5,20,21,23–25] or inclusions, the crack front tends to avoid the obstacles and is deviating from a straight line on a larger scale.

Conclusions

Summarising, it has been shown that a kink-pair mechanism is relevant for *dynamic* fracture of ordered brittle solids at low loads. Crack fronts in general do not form a straight line. Increasing the load results in kink motion, which is more complex. Furthermore, an enhanced roughness of the fracture surfaces is observed. Compared to quasi-static approaches cracks as a matter of principle do not follow minimal energy paths. In the non-equilibrium process the energy dissipation mechanisms play a major role, which complicate the suggested simple kink-pair process of crack advance.

Acknowledgments

Support from the Deutsche Forschungsgemeinschaft under contract number TR 154/25-1 and within the Cluster of Excellence 310 (Simulation Technology) as well as by the European Network of Excellence on Complex Metallic Alloys (NMP3-CT-2005-500140) is gratefully acknowledged. The authors would like to thank the anonymous Referee B of [7], who motivated this paper by his review.

References

[1] A. Seeger, *J. Phys. Colloques*, **42** (1981) C5-201.
 [2] E. Mann, *Phys. Stat. Sol. B*, **144** (1987) 115.
 [3] R. Thomson, C. Hsieh and V. Rana, *J. Appl. Phys.*, **42** (1971) 3154.
 [4] A. A. Griffith, *Philos. Trans. R. Soc. Lond. Ser. A*, **221** (1921) 163.

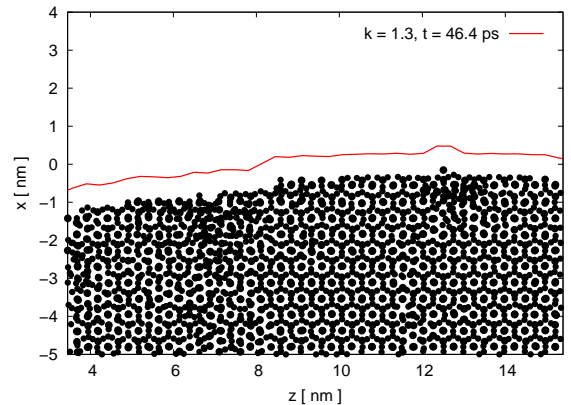


Fig. 5: Crack advancing at a higher load ($k = 1.3$).

- [5] F. Rösch, C. Rudhart, J. Roth, H.-R. Trebin and P. Gumbsch, *Phys. Rev. B*, **72** (2005) 014128.
 [6] F. Rösch, Doctoral thesis <http://elib.uni-stuttgart.de/opus/volltexte/2008/3598/>
 [7] F. Rösch and H.-R. Trebin, *epl*, **85** (2009) 56002.
 [8] T. Zhu, J. Li and S. Yip, *Phys. Rev. Lett.*, **93** (2004) 205504.
 [9] T. Zhu, J. Li and S. Yip, *Proc. R. Soc. A*, **462** (2006) 1741.
 [10] N. Bernstein and D. W. Hess, *Phys. Rev. Lett.*, **91** (2003) 025501.
 [11] G. Csányi, T. Albaret, M. C. Payne and A. De Vita, *Phys. Rev. Lett.*, **93** (2004) 175503.
 [12] M. J. Buehler, A. C. T. van Duin and W. A. Goddard III, *Phys. Rev. Lett.*, **96** (2006) 095505.
 [13] A. Mattoni, M. Ippolito and L. Colombo, *Phys. Rev. B*, **76** (2007) 224103.
 [14] B. R. Lawn, *J. Mater. Sci.*, **10** (1975) 469.
 [15] M. Marder, *J. Stat. Phys.*, **93** (1998) 511.
 [16] J. H. Wernick, *Intermetallic Compounds*, edited by J. H. Westbrook (John Wiley & Sons, Incorporated) 1967, p. 197.
 [17] F. Rösch, H.-R. Trebin and P. Gumbsch, *Int. J. Fracture*, **139** (2006) 517.
 [18] S. J. Zhou, P. S. Lomdahl, R. Thomson and B. L. Holian, *Phys. Rev. Lett.*, **76** (1996) 2318.
 [19] P. Gumbsch, S. J. Zhou and B. L. Holian, *Phys. Rev. B*, **55** (1997) 3445.
 [20] F. Rösch and H.-R. Trebin, *Phys. Rev. B*, **78** (2008) 216201.
 [21] F. Rösch and H.-R. Trebin, *Z. Kristallogr.*, **223** (2008) 827.
 [22] M. Marder, *Comp. Sc. Eng.*, **1** (1999) 48.
 [23] F. Rösch, H.-R. Trebin and P. Gumbsch, *Phil. Mag.*, **86** (2006) 1015.
 [24] P. Ebert, F. Yue and K. Urban, *Phys. Rev. B*, **57** (1998) 2821.
 [25] P. Ebert, M. Feuerbacher, N. Tamura, M. Wollgarten and K. Urban, *Phys. Rev. Lett.*, **77** (1996) 3827.